David Leleu*
Andreas Pfennig

Coalescence Modeling for Design of Technical Equipment

A coalescence model in the context of the ReDrop concept (Representative Drops) is proposed to design technical equipment for separating liquid-liquid dispersions in settlers or extraction columns. A fundamental study of drop interactions has been performed to obtain the complete picture of coalescence. The model proposed accounts for collision frequency of the drops, bouncing probability, and coalescence probability, for which the film-drainage approach is applied. The model proposed allows considering the appropriate formulation for different types of equipment. Especially noteworthy is that the coalescence probability fundamentally differs from the expression of Coulaloglou and Tavlarides, which is frequently used, but which shows inconsistencies at fundamental level.

Keywords: Coalescence, Coalescence modeling, Film drainage, Liquid-liquid dispersion, Phase separation

Received: January 30, 2019; *revised:* May 15, 2019; *accepted:* May 16, 2019

DOI: 10.1002/ceat.201900037

Supporting Information available online

1 Introduction

Liquid-liquid dispersions occur in equipment like continuous settlers or extraction columns. Typically, especially at increased viscosity, a wide drop size distribution can be observed. This polydispersity can lead to a remaining fraction of fine drops found at the equipment outlet. Thus, to properly design technical equipment, the behavior of the drops has to be described accurately also accounting specifically for these fine drops. However, drop behavior differs between different types of equipment. For extraction columns, due to the energy input, turbulences occur that influence the drop motion and especially the probability that drops meet as well as the time they stay in contact. For settlers, the drops sediment without much turbulence driven by buoyancy until they reach a close packed layer where they finally coalesce. These different configurations have various effects on the details of coalescence. Thus, the type of equipment influences the fluid dynamics surrounding the drops, affecting drop collision and, as a consequence, coalescence [1].

Coalescence is especially challenging to describe because it is affected by various characteristics specific to the investigated system. Besides the material properties like surface tension, density, and viscosity, the presence of trace impurities strongly affects coalescence [14]. Especially ionic species induce electrostatic forces at the drops' interface, which can aid or hinder coalescence.

To design technical equipment, the models describing the behavior of the drops need to be implemented in a simulation tool that predicts the overall behavior of the liquid-liquid dispersion. The ReDrop (Representative Drops) concept can be used for this purpose, in which a Monte Carlo algorithm is applied to solve the population-balance equations [1, 26]. In this stochastic approach, the drops generated in the simulation are considered as representative drops. Each individual drop considered is thus representing drops that possess identical characteristics like diameter, height in the equipment, or velocity. Thus, for the coalescence model, individual drops undergoing a coalescence event are considered, where the probability of finding these drops in the volume regarded has to be accounted for separately, taking care, e.g., for the local holdup and drop size distribution.

In simulating a batch settler or an extraction column, this corresponds to regarding a representative cross-sectional area A_{repr} of the equipment, in which the number of representative drops have the identical holdup as the overall dispersed phase in the large system simulated. With holdup and size distribution, the probability for the individual drops can be converted into any desired probability expression, e.g., alternatively characterizing probabilities of drop size classes. Additional effects like the influence of mass transfer on coalescence are beyond the scope of this paper and thus not considered, especially, because until now only qualitative understanding, e.g., of the influence of Marangoni effect, is available.

The goal of the paper is thus to establish a complete coalescence model that can be applied to different types of technical equipment for design purpose. The drop interactions are treated in detail to integrate the effect of trace components in the model and to understand the effect of polydispersity on coales-

David Leleu, Prof. Dr.-Ing. Andreas Pfennig
dleleu@uliege.be
University of Liège, Department of Chemical Engineering – Products, Environment, and Processes (PEPs), Quartier Agora, Allée du Six Août, 11, 4000 Liège – Sart-Tilman, Belgium.

cence. The developed model should consider the concept of representative drops to allow using it also in ReDrop simulations.

2 Simulation Tool

The developed ReDrop tool considers each individual drop from a sufficiently large ensemble of drops present in the system. The vertical motion as well as coalescence events between them is then simulated as time proceeds as described below. The horizontal position of the drops is not evaluated, i.e., it is assumed that the drops are randomly distributed horizontally. As a consequence, special care has to be taken to properly evaluate the contact probability of two drops as a basis to quantify correctly the probability of a coalescence event.

To keep track of local holdup and average variables like local Sauter mean diameter, the equipment is divided into volume elements. The Sauter mean diameter influences the sedimentation velocity and is taken into account in the models, e.g., for sedimentation. The local Sauter mean diameter is also used to evaluate, e.g., characteristics of the drop packing in the close-packed zone.

The physical properties of the system and the simulation parameters like density, viscosity, initial holdup, parameters of the drop size distribution, simulation time step, etc. are made available to the ReDrop program via input files, which are supplied by the user.

At the start of the simulation, the drops are randomly positioned with respect to the height of the batch-settling cell simulated. The relative velocity between the individual drops and the surrounding continuous phase is then determined from the single drop sedimentation model proposed by Henschke coupled to the swarm model of Richardson and Zaki [31, 35]. From the balance for each height element, the continuous-phase flow is obtained which is linearly interpolated within each height element, thus allowing to calculate the absolute velocity of each drop, which is evaluated for each time step in order to determine their individual vertical position in the settling cell. At a certain value of holdup, detailed in Sect. 4.5.1, the dispersion is assumed to be close-packed. In that zone, the drops are continually in direct contact, which influences the contributions relevant for calculating the coalescence probability as described below. The drops that have reached the close-packed zone are assumed to stay in contact, independent of a possible vertical motion of the entire close-packed zone, which is, e.g., induced by coalescence of drops with the major interface. The last drop of the close-packed zone, delimiting this zone from that of free sedimentation, is kept track of, since drops can also enter the close-packed zone by sedimenting past that last drop. If the latter occurs, the drop is sorted into the close-packed zone.

Coalescence of drops with the major interface can occur with all drops that are close enough to the interface. Since the vertical arrangement of the drops is not depicted in the simulation, all drops in the nearest vicinity of the interface are considered the cross-sectional area of which add up to the local holdup at the interface multiplied with A_{repr}. To have the possibility to account for specific packing effects, an additional scaling parameter for that cross-sectional area is included, which will be fitted to systematic future experiments and is assumed to take values close to unity. The exact position of the major interface is tracked adding the volume of the drops that underwent drop-interface coalescence. The coalescence frequency is then evaluated with the model described below between each pair of drops, which are close enough to each other to be able to come into contact, i.e., the center of which differ in vertical position by less than their average diameter. The individual coalescence event is then triggered by comparing the coalescence probability between two drops with a random number as described in [1]. After coalescence has been considered for all drops, the algorithm continues with the next time step for sedimentation.

From the simulations, the time-dependent position of the major interface and the position of the last drop of the close-packed zone are directly obtained. The sedimentation curve is evaluated from the holdup profiles with the help of a user-defined limiting value, e.g., 10 % of the initial phase ratio.

3 Different Principal Approaches to Describe Coalescence

A variety of models to describe coalescence have been proposed, for which recent extensive overviews are available [1, 2, 9, 11]. Here, only those aspects relevant for this work are summarized. Coalescence is a stochastic event that can be quantified by a probability, $p_{coalescence}$, which describes with which probability two drops coalesce, depending on the diameter and the velocity of the drops considered. To quantify $p_{coalescence}$, different modeling approaches have been proposed: the energy model, the critical-velocity model, and the film-drainage model.

In the energy model, it is assumed that the kinetic energy of the drops, E_K[1)], has to overcome an energy barrier characterized by the surface tension, E_σ, [6, 7], leading to an overall description resembling a Boltzmann probability:

$$p_{coalescence} \propto \exp\left(-\frac{E_\sigma}{E_K}\right) \tag{1}$$

This approach has been proposed to describe the coalescence for a turbulent system, e.g., a stirred tank. The energy model states that coalescence is enhanced by a high collision energy.

In the critical-velocity model, the relative velocity of the drops, $v_{relative}$, is compared to a critical velocity, $v_{critical}$, independent of the drop diameter, above which coalescence is assumed not to take place [2, 8]:

$$p_{coalescence} = \min\left(\frac{v_{critical}}{v_{relative}}, 1\right) \tag{2}$$

This model is based on experiments performed on bubble coalescence in turbulent flow [8]. In contrast to the energy

1) List of symbols at the end of the paper.

model, here the coalescence is enhanced for small collision velocity.

In a third approach, it is assumed that a film forms between two colliding drops that meet and that the drainage of this film determines the coalescence probability. Coalescence occurs when the film thickness reaches a critical lower value [2, 3, 10–12]. The coalescence probability is expressed by:

$$p_{\text{coalescence}} = \exp\left(-\frac{t_{\text{coalescence}}}{t_{\text{contact}}}\right) \tag{3}$$

where the coalescence time, $t_{\text{coalescence}}$, describes the time required for coalescence, which is compared to the contact time, t_{contact}, which defines how long the drops stay in contact under the specific fluid-dynamic conditions of the equipment regarded.

To investigate, which model is better suited to describe coalescence, Kamp performed collision experiments between one fixed drop and a moving drop and found that for high relative velocity, the coalescence probability is close to zero [9]. This cannot be described with the energy model, which is thus not applicable for liquid dispersions. On the other hand, Henschke has shown that detailed modeling of phase separation is possible, if coalescence is modeled with the drainage model, which does not just depend on relative drop velocity [12, 21, 31]. This indicates that the drainage model is a good starting point for detailed investigation. This is supported by a variety of studies showing the influence of film drainage on coalescence [2, 3, 10–12] and demonstrating good correlation between experimental results and the film-drainage model [1, 12]. Thus, the film-drainage model is chosen as a basis for further investigation of the coalescence in this study.

4 Coalescence Model Adapted for Technical Equipment

The model described in this section builds on known knowledge as indicated by the references below and introduces new insights, especially for the detailed description of film drainage, the consistent coalescence-probability expression, and including the bouncing probability.

To model coalescence in a simulation, for a drop or a drop class, the coalescence frequency $f_{\text{coalescence}}$ has to be quantitatively described, which represents the number of coalescence event per unit of time between two representative drops. In order to characterize $f_{\text{coalescence}}$, the individual steps occurring during the coalescence event need to be accounted for as indicated schematically in Fig. 1. To allow coalescence between two

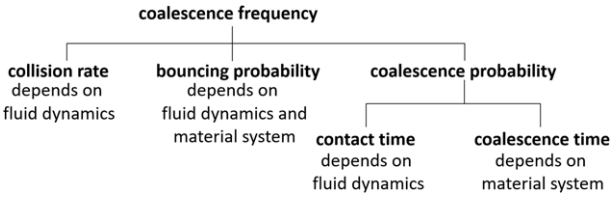

Figure 1. Schematic representation of steps in the coalescence process.

drops, they first need to enter into a collision. The collision between two representative drops can be characterized by a frequency, $f_{\text{collision}}$, indicating how often these drops would meet per unit of time. Once the drops met, they have a chance to coalesce, which is evaluated via the coalescence probability $p_{\text{coalescence}}$, which in turn, in the regarded film-drainage model, depends on the contact time and on the coalescence time.

The coalescence frequency is thus frequently described as the product of collision frequency and coalescence probability [1, 9]:

$$f_{\text{coalescence}} = f_{\text{collision}} p_{\text{coalescence}} \tag{4}$$

The collision frequency and the contact time depend on the fluid dynamics surrounding the drops and thus on the type of equipment. Indeed, the turbulences are stronger in extraction columns compared to continuous settlers affecting the corresponding terms. The coalescence time, on the other hand, solely depends on the material properties and the details of interfacial interactions including effects of trace components.

In the general case, Eq. (4) has to be extended for an additional effect observed experimentally. Kamp [9] as well as Lehr and Mewes [8] evaluated the coalescence probability between individual drops and bubbles, respectively. The authors found that for high relative velocity the coalescence probability is close to zero. Thus, if their relative velocity exceeds a critical value, the drops can directly bounce when they meet. If their relative velocity is relatively small, the drops stay in contact, follow their mutual curvature, and during this time the coalescence process can take place. To account for this effect, a bouncing probability, p_{bouncing}, is included in Eq. (4), leading to:

$$f_{\text{coalescence}} = f_{\text{collision}} \left(1 - p_{\text{bouncing}}\right) p_{\text{coalescence}} \tag{5}$$

The different variables influencing the coalescence frequency will be detailed in the following sections.

4.1 Collision Frequency

Different phenomena induce drop collisions in liquid-liquid dispersions, depending on the type of equipment [2]. First of all there has to be a chance that the drops can meet geometrically. If the drops experience essentially random motion, e.g., being induced by the turbulence in extraction columns, the collision frequency $f_{\text{turbulence}}$ can be described in analogy to the kinetic gas theory, assuming that the drops behave like spheres [32]:

$$f_{\text{turbulence}} = C_{\text{coll,turbulence}} (d_1 + d_2)^2 \Psi^{1/3} \sqrt{d_1^{2/3} + d_2^{2/3}} \times \frac{1}{(1+\varepsilon)} \tag{6}$$

where d_i is the diameter of the drops and Ψ is the energy dissipation, which has to be described properly for each type of extraction column. $C_{\text{coll,turbulence}}$ is a parameter dependent on the type of the column. This equation also accounts for the geometric chance of two drops meeting via the holdup.

For continuous settlers, on the other hand, the drop motion is caused mainly by their vertical sedimentation, the collision being mostly induced by their buoyancy [3, 34]. In large settlers additionally large-scale flow structures can occur. Since their velocity will be of the order of the overall flow velocity of the phases, which is typically around 1 cm s^{-1}, and their dimensions are large, their effect on relative drop motion on the scale of mm will be negligible and thus they do not contribute to drop-approach velocity. Brownian motion can induce also a random contribution in the trajectories of the drops, which is negligible for drops below 10 µm diameter [37]. Since in technical settlers typical drop diameters in an initial dispersion are found above 50 µm, Brownian motion can be neglected here as well.

Thus, for the particular case of batch settler, the motion of the drops is assumed to be vertical. To describe the collision frequency of vertically moving drops, two freely sedimenting drops can be considered as depicted in Fig. 2. The drops move in the representative volume of the settler with a bottom area of A_{repr}. Their vertical positions is h_i. The drops shown can meet, if their centers lie in the collision cylinder indicated, leading to a geometric probability that the drops meet being:

$$p_{coll} \propto \frac{\pi(d_1 + d_2)^2}{4A_{repr}} \tag{7}$$

Eq. (7) corresponds to the particular case where the drops are at the same height. In general, especially if the position of the drops is accessible in modeling, the collision probability depends on the height difference between the drops, which leads to:

$$p_{coll} = \frac{\pi\left((d_1 + d_2)^2 - 4(h_1 - h_2)^2\right)}{4A_{repr}} \tag{8}$$

This probability is appropriate, if the vertical motion of individual drops is characterized for each time step. If, instead, the overall collision is regarded, Eq. (8) can be averaged over the possible contact geometries, e.g., drops meeting along their central axis or just touching in passing. This overall collision probability is thus expressed by:

$$p_{coll} = \frac{\pi(d_1 + d_2)^2}{6A_{repr}} \tag{9}$$

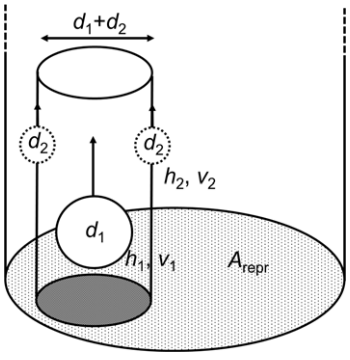

Figure 2. Sketch describing the collision phenomenon in a batch settling experiment.

These considerations show that the geometric probabilities of two drops to meet depends on the specifics of how the equipment and drops are represented in the simulation. The corresponding equation also needs to take into account, if the drops are regarded individually or as class in a drop size distribution and has to be adjusted correspondingly. For example, if drop classes are regarded, the local holdup needs to be included in defining the collision probability because the probability of a drop in one class to meet one of another class also depends on the product of the holdup of both drop size classes. This is not required here, where each individual drop is a representative for drops of equal properties.

The geometric probability then has to be corrected for the so-called free volume effect, which expresses that in the vicinity of a drop the free volume is reduced, which tends to increase the number of collision [1]. Again assuming that the drops behave like an ensemble of spheres, this effect can be quantified with the radial distribution function at contact. While this effect has already been accounted for based on monodispersed drop size distributions [1, 2], in technical systems polydispersity is the typical case [6, 33]. Thus, here the hard-sphere model of Boublik [4] and Mansoori et al. [5] has been considered:

$$\gamma = 1 + C_{BMCSL}\left(\frac{1}{1-\varepsilon} + \frac{3\xi d_1 d_2}{(1-\varepsilon)^2(d_1 + d_2)} + \frac{2\xi d_1^2 d_2^2}{(1-\varepsilon)^3(d_1 + d_2)^2} - 1\right) \tag{10}$$

with

$$\xi = \sum_i \frac{\pi x_i d_i^2}{6} \tag{11}$$

where x_i is the number fraction of drops of a diameter d_i. Here, C_{BMCSL} is an adjustable parameter, which scales this factor. It has been shown that for extraction columns the full effect has to be taken into account. For settlers a reduced influence is expected, since a random influence on drop motion is not predominant and only slightly induced by the drop swarm hindering the sedimentation of individual drops.

The correction factor, γ, can be placed in front of Eqs. (8) and (9) to take into account the effect of the free-volume reduction.

As a next factor, the contribution of relative velocity on the collision frequency has to be taken into account. If the equipment is as usual subdivided into height elements of height Δh, the probability of two drops to meet will be proportional to $v_{relative}/\Delta h$.

The collision frequency for drops moving due to buoyancy, $f_{buoyancy,average}$, is thus:

$$f_{buoyancy,average} = C_{coll,buoyancy}\frac{\gamma p_{coll} v_{relative}}{\Delta h} \tag{12}$$

The adjustable parameter $C_{coll,buoyancy}$ collects all the geometric and other proportionality factors mentioned previously.

Finally, in the general case, buoyancy and turbulence both contribute to overall collision frequency [1]:

$$f_{\text{collision}} = f_{\text{buoyancy}} + f_{\text{turbulence}} \tag{13}$$

Drops located in a close-packed layer are always in contact. In this case, only the geometric considerations need to be accounted for to characterize the probability with which drops of specific diameter are in contact. All other contributions are unity.

4.2 Bouncing Probability

After two drops collided, their bouncing probability has to be considered. The experimental data of Kamp [9], who analyzed the interaction of a drop hanging at the tip of a capillary in the continuous phase, which is hit by a drop produced with a syringe at different relative position with respect to the first drop, are presented in Fig. 3. These data and the study of bubble coalescence of Lehr and Mewes [8] suggest that the bouncing probability can be represented by a step function as an approximation:

$$p_{\text{bouncing}} = \begin{cases} 1 \text{ if } v_{\text{relative}} \le v_{\text{critical}} \\ 0 \text{ otherwise} \end{cases} \tag{14}$$

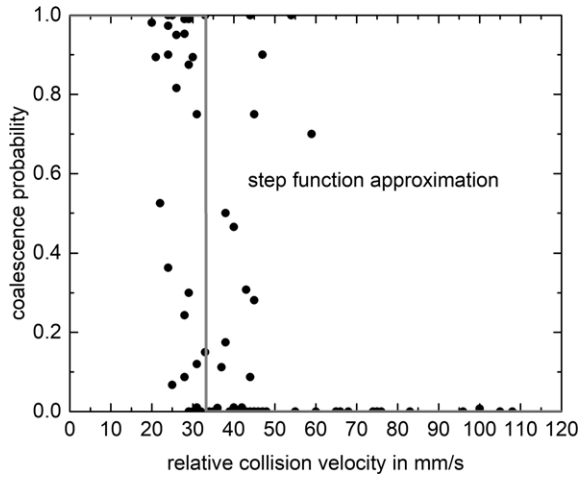

Figure 3. Data of Kamp [9] showing the influence of the collision velocity on the coalescence probability.

In a gravity settlers, the bouncing probability can be assumed to be negligible due to the small velocity difference between sedimenting drops. However, for extraction columns, this variable needs to be accounted for, because local velocities and shear rates of continuous phase including turbulences can be significant [1] as, e.g., in stirred columns [36]. From a balance between the kinetic and the interfacial tension forces, the following can be found:

$$v_{\text{critical}} = \sqrt{\frac{R_{\text{eq}}^3 \Delta\rho g^2}{3\sigma}} \tag{15}$$

where R_{eq} is the equivalent radius of the two considered drops:

$$R_{\text{eq}} = \frac{d_1 d_2}{d_1 + d_2} \tag{16}$$

4.3 Coalescence Probability

As a next step, if the drops stay in contact after the collision, the coalescence probability has to be characterized. As concluded in Sect. 2, coalescence probability between two representative drops can best be expressed by the film-drainage model, in which the contact time is compared to the coalescence time through a Boltzmann probability function. The equation mostly used to describe coalescence probability in extraction equipment is the model of Coulaloglou and Tavlarides [10], already introduced as Eq. (3).

In order to understand how the coalescence time and the contact time are related in the expression of the coalescence probability, the coalescence phenomenon can be regarded more closely. Conceptually, the overall contact time t_{contact} can be subdivided into n time steps, Δt. For each time step, the probability of non-coalescence can be characterized as $p_{\text{non-coalescence},\Delta t}$. Then, assuming that the probability is independent of the specific Δt regarded, for nΔt the following has to hold:

$$p_{\text{non-coalescence,n}\Delta t} = \left(p_{\text{non-coalescence},\Delta t}\right)^n \tag{17}$$

Only an exponential function fulfills this boundary condition, which requires the overall non-coalescence efficiency to be written as:

$$p_{\text{non-coalescence}} = \exp\left(-\sum_n \frac{\Delta t}{t_{\text{coalescence}}}\right) \tag{18}$$

In principle, this equation would also allow to regard individual probabilities of non-coalescence at different time steps, characterized by varying $t_{\text{coalescence}}$. If it is again assumed that all $p_{\text{non-coalescence},\Delta t}$ are identical for the overall contact time, the coalescence probability results:

$$p_{\text{coalescence}} = 1 - \exp\left(-\frac{t_{\text{contact}}}{t_{\text{coalescence}}}\right) \tag{19}$$

Varying non-coalescence probabilities can here be accounted for by regarding the $t_{\text{coalescence}}$ as an effective overall coalescence time. Eq. (19) clearly differs from different film drainage models [28–30] and especially from the known equation of Coulaloglou and Tavlarides, Eq. (3) [10]. The new expression in Eq. (19) is especially consistent in simulations, where time is subdivided into time steps, yielding consistent results. If the expression of Coulaloglou and Tavlarides, Eq. (3), is used in a simulation per time step, then factually the probability of drops surviving behaves as Eq. (17). As a consequence, effectively a behavior as Eq. (19) is used. Thus, in a simulation with time-step resolution the description differs from one, where the inte-

gral collision is regarded via $t_{contact}$. Thus, only with Eq. (19) independent of regarding the overall collision or dividing it into time steps, consistent description is achieved.

4.4 Contact Time

A model describing the overall contact time between two drops, used by several authors, takes the form [1, 9, 10]:

$$t_{contact} = \frac{(d_1 + d_2)^{2/3}}{\Psi^{1/3}} \tag{20}$$

which accounts for isotropic Kolmogorov turbulences. The energy dissipation can then be linked to the relative velocity of the drops by [9, 10]:

$$v_{relative} = \sqrt{2}(\Psi(d_1 + d_2))^{1/3} \tag{21}$$

which, combined with Eq. (20), yields:

$$t_{contact} = \sqrt{2}\frac{d_1 + d_2}{v_{relative}} \tag{22}$$

Eq. (22) is supported by the simulation of the relative motion of the drops as described in the Supporting Information. The equation is thus chosen to model the contact time between two drops. However, for extraction columns, Eq. (20) can be used instead of Eq. (22), together with an appropriate description of energy dissipation for the column type considered.

4.5 Coalescence Time

During drop contact, a force acts between the two drops in contact finally possibly leading to coalescence. The film occurring between the drops decreases in thickness over time, which implies a drainage flow of continuous phase out of this film. The fluid-dynamic force, induced by this flow, is balanced by the driving force acting between the drops. The coalescence time is thus the time required to reduce that film until a critical thickness is reached below which coalescence is induced. In modeling this process, drop deformation and interface mobility have to be taken into account [2, 13, 21].

The mobility of the interface may, e.g., be hindered by the presence of surfactants or by high viscosity of the dispersed phase [1, 11]. For technical systems, the drop interface can be assumed immobile due to the impurities typically present. For other situations, the corresponding expressions have been collected by Kopriwa [13].

The details of various models describing the film drainage have been studied by Henschke [21]. He could show that models assuming rigid spherical drops [2] or a film of constant thickness, the so-called disk model, are not able to properly describe reality in an extraction equipment. Experiments actually indicate that drop deformation during the film drainage leads to the formation of a dimple [11, 12, 17]. A dimple is characterized by the thickness of the film between the drops not being constant. It has a maximum thickness along the central axis between the drops and has a thinner rim with a radius R_F. As a consequence, film drainage is mainly limited by the flow through this narrow slit, which on the other hand is the location, where film drainage ruptures when the minimum thickness decrease below a critical value. Experiments actually show that this dimple is not radially symmetric, which influences the drainage of the dimple. Henschke thus proposed a model including also this asymmetry leading to faster drainage than in the symmetrical case by superimposing the model for symmetrical dimple drainage with an asymmetric action of the driving force. This asymmetry is characterized by a dimensionless parameter r_s^*, which characterizes how asymmetric the force acts [12]:

$$t_{coalescence} = \frac{3\pi^2 \mu R_F R_a^{3/2}}{2F_{driving} r_s^* \sqrt{h_{critical}}} \tag{23}$$

This coalescence parameter varies between 0 and 1. Here, μ is the viscosity of the continuous phase, R_a is the curvature of the dimple, and $h_{critical}$ denotes the critical thickness below which film rupture occurs resulting in the two drops joining. The parameters and variables in this model will be discussed in some detail in the following for different situations.

4.5.1 Geometric Dimple Characteristics

The geometric dimple characteristics depend on the physicochemical properties of the solvent like surface tension and on the force acting between the drops. If two freely sedimenting drops are considered that come into contact with a dimple forming between them, the dimple radius can be obtained from a force balance between the fluid-dynamic force and the force induced by surface tension, characterized by the Young-Laplace force, $F_{Young\text{-}Laplace}$ [11]:

$$F_{Young-Laplace} = \frac{\pi R_F^2 \sigma}{R_{eq}} = F_{fluid-dymanic} \tag{24}$$

where σ represents the interfacial tension. Since the fluid-dynamic force is also balanced with the driving force, Eq. (24) leads to:

$$R_F = \sqrt{\frac{F_{driving} R_{eq}}{\pi\sigma}} \tag{25}$$

Here, also coalescence with the major interface can be discussed. To describe coalescence of a drop with the interface, Eq. (23) can be applied as well, but it has to be taken into account that the dimple radius will be larger by a factor of $\sqrt{3}$ as compared to Eq. (25) [12, 21].

If finally dimple curvature is assumed proportional to the equivalent drop diameter, with Eq. (23) it follows:

$$t_{coalescence} = \frac{3C_{dimple}^{3/2}\pi^{3/2}\mu R_{eq}^2}{2r_s^* \sqrt{F_{driving}\sigma h_{critical}}} \tag{26}$$

where C_{dimple} is the parameter scaling the dimple curvature regarding the drop radius.

A different situation occurs, if two drops are in contact in a close-packed zone, because the hydrostatic pressure of the surrounding drops exerts the driving force for film drainage, simultaneously increasing the surface area between the drops and thus the dimple radius, affecting also dimple curvature. To model the behavior, Henschke [21] described the drop deformation, accounting for the hydrostatic pressure acting:

$$R_a = 0.5 d_{3,2}\left(1 - \sqrt{1 - \frac{4.7}{La + 4.7}}\right) \tag{27}$$

$$R_F = 0.3025 d_{3,2}\sqrt{1 - \frac{4.7}{La + 4.7}} \tag{28}$$

where La is the Laplace number:

$$La = \frac{\Delta\rho g h_{d,cpz} d_{3,2}}{\sigma} \tag{29}$$

$\Delta\rho$ the density difference between the phases, g is the gravitational acceleration, and $d_{3,2}$ is the local Sauter mean diameter around the considered drop, which can be determined from its value in each height element. $h_{d,cpz}$ is the relative height of the drop in the close-packed zone. Thus, the hydrostatic pressure applied on this drop is:

$$\Delta P_{hy} = \varepsilon g \Delta\rho h_{d,cpz} \tag{30}$$

Here, ε is the local holdup. In this model, monodispersed drops are assumed, which means that squeezing sets in beyond a holdup of spherical close packing, i.e., 0.74. This value thus corresponds to the drop holdup where the drops are just entering into the close-packed zone.

To generalize for polydisperse systems, the initial packing of the monodispersed sample was compared to the model of Corwin et al. [25], with which the packing of polydisperse frictionless spheres can be evaluated. It turns out that for drops with a radius below 1 mm and a variance of the drop size distribution below 50 %, which are typical values for drops entering the close-packed zone, the holdup varies between 70 % and 80 %. Thus, a value of 0.74 appears to be a good estimate for the limiting holdup also for polydisperse drops.

4.5.2 Driving Force

The force acting on the drops leading to film drainage depends on the drops' situation. For example, in batch settling, the driving force differs between the sedimentation zone and the close-packed zone. For freely sedimenting drops, the difference in buoyancy force between the two drops is the driving force for the coalescence:

$$F_{driving} = \frac{\pi\Delta\rho g(d_1^3 - d_2^3)}{6} \tag{31}$$

where drop 1 is assumed to be larger than drop 2.

In the close-packed zone, coalescence between drops as well as drops and interface induce an excess of continuous phase that has to flow between the drops. A pressure drop thus occurs in the close-packed zone which acts in the opposite direction as the hydrostatic pressure. The driving force for coalescence of a drop in the close-packed zone is thus the sum of both contributions:

$$F_{driving} = \frac{4\left(\Delta P_{hy} + \Delta P_{flow}\right)}{\pi d^2} \tag{32}$$

The flow of continuous phase through the close-packed zone is not constant because coalescence occurs between the drops and the interface and among drops leading to increasing drop size resulting in more deformed drops, which in turn means less continuous phase between the drops remaining. To evaluate the pressure drop due to this non-constant flow of continuous phase, ΔP_{flow}, the differential form of the Carman-Kozeny equation [24] can be regarded:

$$\frac{dP_{flow}}{dh} = -\frac{180\varepsilon^2\mu}{(1-\varepsilon)^3 d_{3,2}^2} u(h) \tag{33}$$

which is then integrated along the close-packed zone to obtain the pressure drop at each height, assuming a linear velocity profile within each height element considered and applying the Sauter mean diameter of that height element.

In extraction columns the driving force is induced by turbulences. Coulaloglou and Tavlarides assume the driving force to be "proportional to the mean-square velocity difference at either ends of the eddy" [10]:

$$F_{driving} \sim \rho_c \Psi^{2/3}(d_1 + d_2)^{2/3}\left(\frac{d_1 d_2}{d_1 + d_2}\right)^2 \tag{34}$$

Thus, combining Eqs. (31, 32, 34) with Eq. (22) allows to model the coalescence time for all different situations considered.

4.5.3 Coalescence Time Parameters

The critical height, $h_{critical}$, is the minimum film thickness below which the film of the dimple ruptures and the final step of coalescence sets in and the drops join. Henschke avoided this parameter by an elegant but not straightforward elimination. This parameter appears in the developed model and is fixed arbitrarily to 10^{-8} m.

The final parameter of the coalescence model, the asymmetry parameter r_s^*, has to be fitted to experimental data, e.g., utilizing a standardized settling cell as proposed by Henschke, to account also for the effects of trace impurities [12].

5 Materials and Methods

5.1 Experimental Setup

Batch settling experiments have been performed to validate the numerical approach and thus the coalescence model. The

experiments are performed in a stirring cell similar to the one developed by Henschke. The cell is made of a glass cylinder of 185 mm height and a diameter of 83 mm. Two shafts with four stirrers on each shaft, each with four tilted blades, are used for stirring to generate the initial dispersion. They are connected with a gearbox such that they are counter-rotating during stirring. This has the advantage that during at most few seconds after switching off the stirrers the dispersion comes to rest without the need of baffles. The gearbox is driven by a stirrer motor. The dispersion is generated by stirring for 30 s at 800 min^{-1}.

The cell is illuminated from behind with an LED panel. A camera (canon EOS 1300D) is placed in front in order to record a video of the settling. The video is then analyzed with Matlab. On each frame, the grey level is averaged horizontally resulting in a vertical pixel line with height-dependent grey level from each frame of the video. The lines are placed beside each other in order to visualize the complete evolution of the separation. In addition, the initial drop size distribution is measured with the SOPAT probe (SOPAT-VR-Sc, SOPAT, Berlin). Matlab is then also used to determine the coalescence and sedimentation curves, where the user can adjust the applied grey-scale levels. The numerical parameters of the ReDrop software are then fitted to those experimental data.

5.2 Materials

The two-phase system used is generated from distilled water, hexane (provided by VWR, batch no. 18Z1660), and ethylene glycol (VWR, batch no. 18H024016). This system is used at its iso-optical tie line, which is determined by successive addition of water. Methylene blue (VWR, batch no. 99C050005) is added to the water at a concentration of 1.8 mg L^{-1}. The distilled water is produced with the GFL 2001/4 unit (GFL, Burgwedel, Germany).

The density and the viscosity are measured after saturation with the equipment DSA 5000M combined with Lovis 2000ME (Anton Paar, Graz, Austria). The interfacial tension is determined with the equipment Lauda TD2. The properties of each phase are summarized in Tab. 1.

Table 1. Physicochemical properties of the system chosen for the settling experiments.

	Aqueous phase	Organic phase
Density [kg m^{-3}]	1053.9	660.1
Viscosity [mPa s]	3.0	0.32
Interfacial tension [mN m]	19.1	

6 Results

First results are illustrated in Fig. 4 obtained with a ReDrop-based simulation for the system describing the material system mentioned in Sect. 5.2. The results of this drop-based approach demonstrate that some particularities, typically observed experimentally, can be understood. In Fig. 4, in addition to the close-packed zone, which is delimited by the white line, a densely packed zone can be found, which corresponds to free sedimentation but in a regime of high holdup. This overall leads to a significant variation of holdup in the region, previously regarded as 'close-packed'. If the coalescence parameter is increased to faster coalescence between sedimenting drops, this leads to a curved shape of the sedimentation zone.

If additionally the initial drop size is reduced to, e.g., 50 µm, which has also been observed as starting drop size experimentally, a lag time can be seen, which results from the small drops of the initial dispersion first needing to coalesce until the drops reach a size of typically around 0.2 mm, which is then large enough to have a significant sedimentation velocity. Thus, drop-based simulation allows generating detailed understanding of process fundamentals.

7 Conclusion

These considerations show that the coalescence frequency can rather generally be described based on the concept schematically depicted in Fig. 1. Each of the different contributions can quite naturally be described by an expression specifically

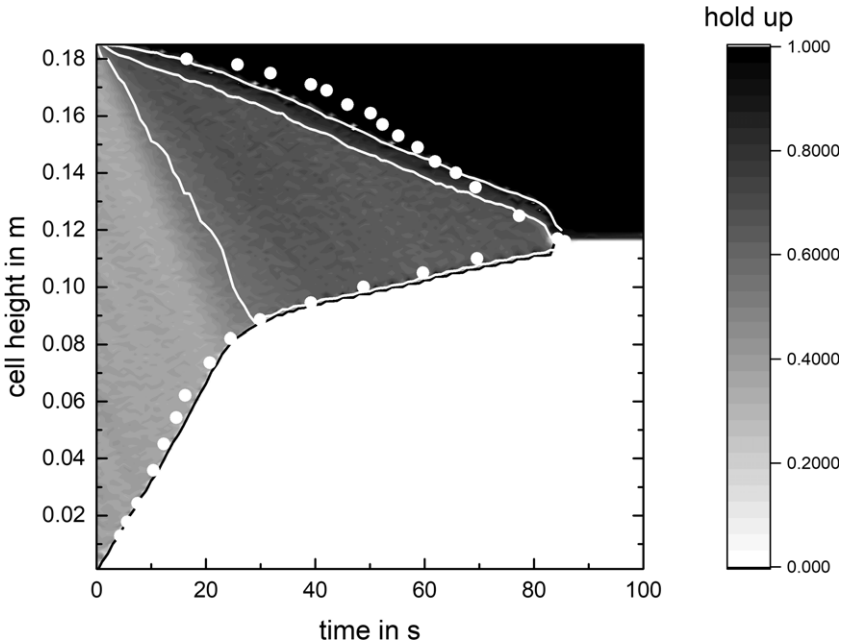

Figure 4. Holdup profile obtained with a ReDrop simulation of a lab-scale batch settling experiment, log normal starting drop size distribution (mean: 620 µm, standard deviation 95 µm), $C_{coll,turbulence} = 0$, $C_{BMCSL} = 0$, $C_{coll,buoyancy} = 0.17$, $r_s^* = 0.013$.

adapted to the studied piece of equipment, i.e., settler or extraction column, where the typical contributions are summarized in Tab. 2. It should be emphasized that the coalescence time is quantified based on a generic equation depending on the driving force, which affects the dimple properties and thus the coalescence process. Nevertheless, this model structure allows consistent evaluation for very different conditions. Also, the developed equation describing the coalescence probability, fundamentally differing from that of Coulaloglou and Tavlarides, now allows for a consistent model for different simulation approaches.

Table 2. Different contributions of the coalescence model allow characterization of a wide variety of cases in a consistent way. This applies to drop-drop as well as to drop-interface coalescence, taking the appropriate dimple radius into account.

Application contributions	Freely sedimenting drops	Close-packed layer of drops	Extraction column
Collision rate	Induced by buoyancy force	Only geometric contribution	Induced by turbulence and by buoyancy force [1]
Bouncing probability	Negligible	Does not exist	Induced by turbulence
Driving force for the film drainage	Buoyancy force + DLVO force	Hydrostatic pressure + DLVO force	Turbulence force + buoyancy force + DLVO force
Coalescence time	Dimple model with immobile interface		
Contact time	Related to the relative velocity	Always in contact	Related to the energy dissipation [1, 11]

As a next step, the interaction forces between interfaces can be regarded in order to evaluate simulation parameters as $h_{critical}$. One description of these forces is the DLVO (Derjaguin, Landau, Verwey, Overbeek) theory, which accounts for Van-der-Waals attraction between the drops and electrostatic repulsion between the interfaces [15, 16]. As indicated in Fig. 5 for an example system, under appropriate conditions the net force is repulsive at larger distances, hindering coalescence. Thus, an energy barrier has to be overcome to reach coalescence. A promising property of the DLVO theory is the dependence of the net force on the type and concentration of salt in the system, of which it is known that they can strongly influence coalescence [1, 13, 14]. This influence has already previously been realized and described including the DLVO theory, which has empirically been introduced [6], but not consistently been studied. Thus, in future work, this salt influence will be systematically studied, e.g., assuming in a first approach that $h_{critical}$ can be related to the first root of the DLVO force.

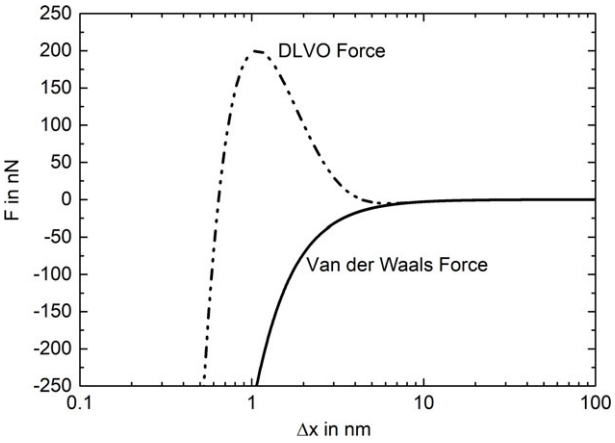

Figure 5. DLVO and Van der Waals forces for a standard system in the presence of ions.

Acknowledgment

The project has partially been supported by the Federal Ministry for Economic Affairs and Energy of Germany, project no. 01168585/1, in the context of the ERICAA project and by the F.R.S.-FNRS – Fonds de la Recherche Scientifique, project no. J011517F.

The authors have declared no conflict of interest.

Symbols used

A	[m^2]	area
d	[m]	diameter
E	[J]	energy
f	[s^{-1}]	frequency
F	[N]	force
g	[$m\ s^{-2}$]	gravitational acceleration
h	[m]	height
La	[–]	Laplace number
N	[–]	number of particles
p	[–]	probability
P	[Pa]	pressure
R	[m]	radius
r	[–]	coalescence parameter
t	[s]	time
u	[$m\ s^{-1}$]	continuous phase velocity
v	[$m\ s^{-1}$]	drop velocity
V	[m^3]	volume

Greek letters

γ	[–]	factor taking into account the free volume reduction of the drops
Δ	[–]	step
ε	[–]	local holdup
μ	[Pa s]	dynamic viscosity of the continuous phase

ξ_2	[m^{-1}]	Boublik Mansoori parameter 1
ξ_3	[–]	Boublik Mansoori parameter 2
ρ	[$kg\,m^{-3}$]	density
σ	[Nm]	surface tension
Ψ	[m^2s^{-3}]	energy dissipation

Subscripts

a	drop
BMCSL	Boublik Mansoori
c	continuous phase
F	contact area of the dimple
i	drop number *i*
K	kinetic

Abbreviations

coll	collision
DLVO	Derjaguin, Landau, Verwey, Overbeek
eq	equivalent
cpz	close-packed zone
hy	hydrostatic
repr	representative

References

[1] N. Kopriwa, A. Pfennig, *Solvent Extr. Ion Exch.* **2016**, *34 (7)*, 622–642. DOI: https://doi.org/10.1080/07366299.2016.1244392

[2] Y. Liao, D. Lucas, *Chem. Eng. Sci.* **2010**, *65 (10)*, 2851–286. DOI: https://doi.org/10.1016/j.ces.2010.02.020

[3] M. J. Prince, H. W. Blanch, *AIChE J.* **1990**, *36 (10)*, 1485–1499. DOI: https://doi.org/10.1002/aic.690361004

[4] T. Boublík, *J. Chem. Phys.* **1970**, *53*, 471–472. DOI: https://doi.org/10.1063/1.1673824

[5] G. A. Mansoori, N. H. Carnahan, K. E. Starling, T. W. Jr. Leland, *J. Chem. Phys.* **1971**, *54 (4)*, 1523–1525. DOI: https://doi.org/10.1063/1.1675048

[6] H. Sovová, *Chem. Eng. Sci.* **1981**, *36 (9)*, 1567–1573. DOI: https://doi.org/10.1016/0009-2509(81)85117-2

[7] W. J. Howarth, *Chem. Eng. Sci.* **1964**, *19 (1)*, 33–38. DOI: https://doi.org/10.1016/0009-2509(64)85003-X

[8] F. Lehr, D. Mewes, *Chem. Eng. Sci.* **2001**, *56 (3)*, 1159–1166. DOI: https://doi.org/10.1016/S0009-2509(00)00335-3

[9] J. Kamp, M. Kraume, *Chem. Eng. Sci.* **2016**, *156*, 162–177. DOI: https://doi.org/10.1016/j.ces.2016.08.028

[10] C. A. Coulaloglou, L. L. Tavlarides, *Chem. Eng. Sci.* **1977**, *32 (11)*, 1289–1297. DOI: https://doi.org/10.1016/0009-2509(77)85023-9

[11] A. K. Chesters, *Chem. Eng. Res. Des.* **1991**, *69 (A4)*, 259–270.

[12] M. Henschke, L. H. Schlieper, A. Pfennig, *Chem. Eng. J.* **2002**, *85 (2–3)*, 369–378. DOI: https://doi.org/10.1016/S1385-8947(01)00251-0

[13] N. Kopriwa, *Quantitative Beschreibung von Koaleszenzvorgängen in Extraktionskolonnen*, Ph.D. Thesis, RWTH Aachen University **2013**.

[14] A. Pfennig, A. Schwerin, *Ind. Eng. Chem. Res.* **1998**, *37 (8)*, 3180–3188. DOI: https://doi.org/10.1021/ie970866m

[15] G. B. Webber, A. E. Scott, G. W. Stevens, F. Greiser, R. R. Dagastine, D. Y. C. Chan, *Soft Matter* **2008**, *4*, 1270–1278. DOI: https://doi.org/10.1039/b717303b

[16] J. Kamp, M. Kraume, *Chem. Eng. Sci.* **2015**, *126*, 132–142. DOI: https://doi.org/10.1016/j.ces.2014.11.045

[17] D. Y. C. Chan, E. Klaseboer, R. Manica, *Soft Matter* **2011**, *7*, 2235–2264. DOI: https://doi.org/10.1039/C0SM00812E

[18] G. D. M. MacKay, S. G. Mason, *Can. J. Chem. Eng.* **1963**, *41 (5)*, 203–212. DOI: https://doi.org/10.1002/cjce.5450410504

[19] S. Hartland, *Chem. Eng. Sci.* **1969**, *24 (3)*, 611–613. DOI: https://doi.org/10.1016/0009-2509(69)85032-3

[20] Y. A. Buevich, E. K. Lipkina, *Colloid. J. USSR* (in English) **1978**, *40 (2)*, 167–171.

[21] M. Henschke, *Dimensionierung liegender Flüssig-flüssig-Abscheider anhand diskontinuierlicher Absetzversuche*, Ph.D. Thesis, RWTH Aachen University **1995**.

[22] R. M. MacAvoy, R. C. Kintner, *J. Colloid Sci.* **1965**, *20 (2)*, 188–190. DOI: https://doi.org/10.1016/0095-8522(65)90009-7

[23] J. Ayesteràn, N. Kopriwa, F. Buchbender, M. Kalem, A. Pfennig, *Chem. Ing. Tech.* **2015**, *38*, 1894–1900. DOI: https://doi.org/10.1002/ceat.201500097

[24] *Particle Technology and Separation Processes*, 5th ed. (Eds.: J. F. Richardson, J. H. Harker, J. R. Backhurst), Coulson and Richardson's Chemical Engineering, Vol. 2, Butterworth Heinemann, Oxford **2002**.

[25] E. Corwin, M. Clusel, A. Siemens, J. Brujic, *Nature* **2009**, *460*, 611–615. DOI: https://doi.org/10.1038/nature08158

[26] N. Kopriwa, F. Buchbender, J. Ayesterán, M. Kalem, A. Pfennig, *Solvent Extr. Ion Exch.* **2012**, *30 (7)*, 683–723. DOI: https://doi.org/10.1080/07366299.2012.700598

[27] J. W. Kim, W. K. Lee, *J. Chem. Eng. Jpn.* **1987**, *20 (5)*, 448–453. DOI: https://doi.org/10.1252/jcej.20.448

[28] E. Cockbain, T. McRoberts, *J. Colloid Sci.* **1953**, *8 (4)*, 440–451. DOI: https://doi.org/10.1016/0095-8522(53)90028-2

[29] T. Gillespie, E. K. Rideal, *Trans. Faraday Soc.* **1956**, *52*, 173–183. DOI: https://doi.org/10.1039/tf9565200173

[30] G. Z. Yu, Z. S. Mao, *Chem. Eng. Technol.* **2004**, *27 (4)*, 407–413. DOI: https://doi.org/10.1002/ceat.200401884

[31] M. Henschke, *Auslegung pulsierter Siebboden-Extraktionskolonnen*, Habilitation, RWTH Aachen University **2003**.

[32] N. F. Carnahan, K. E. Starling, *J. Chem. Phys.* **1969**, *51 (2)*, 635–636. DOI: https://doi.org/10.1063/1.1672048

[33] S. Sajjadi, N. Zerfa, B. W. Brooks, *Chem. Eng. Sci.* **2001**, *57*, 663–675. DOI: https://doi.org/10.1016/S0009-2509(01)00415-8

[34] S. Hartland, D. K. Vohra, *Chem. Ing. Tech.* **1978**, *50 (9)*, 673–682. DOI: https://doi.org/10.1002/cite.330500906

[35] J. F. Richardson, W. N. Zaki, *Trans. Inst. Chem. Eng.* **1954**, *8*, 65–73. DOI: https://doi.org/10.1016/0009-2509(54)85015-9

[36] F. Buchbender, *Single-Drop-Based Modelling of Drop Residence Times in Kuhni Columns*, Ph.D. Thesis, RWTH Aachen University **2003**.

[37] H. Speth, *Ein neues Modell zur Auslegung von Faserbett-Koaleszenzabscheidern*, Ph.D. Thesis, RWTH Aachen University **2004**.

